Discrimination of Cognate and Noncognate Substrates at the Active Site of Class I Lysyl-tRNA Synthetase †

ARTICLE *in* BIOCHEMISTRY · APRIL 2006

Impact Factor: 3.02 · DOI: 10.1021/bi0523005 · Source: PubMed

5 AUTHORS, INCLUDING:

Mette Praetorius-Ibba
The Ohio State University
28 PUBLICATIONS **2,376** CITATIONS
SEE PROFILE

Sandro Ataide
University of Sydney
17 PUBLICATIONS **515** CITATIONS
SEE PROFILE

Michael Ibba
The Ohio State University
164 PUBLICATIONS **5,450** CITATIONS
SEE PROFILE

Published in final edited form as:
Biochemistry. 2006 March 21; 45(11): 3646–3652. doi:10.1021/bi0523005.

Discrimination of cognate and noncognate substrates at the active site of class I lysyl-tRNA synthetase†

Shiming Wang‡, **Mette Prætorius-Ibba**‡,§, **Sandro Ataide**‡, **Hervé Roy**‡, and **Michael Ibba**‡,||,*

‡ *Department of Microbiology, The Ohio State University, Columbus, Ohio 43210, USA*

|| *Ohio State Biochemistry Program, The Ohio State University, Columbus, Ohio 43210, USA*

Abstract

The aminoacyl-tRNA synthetases are divided into two unrelated structural classes, with lysyl-tRNA synthetase (LysRS) the only enzyme represented in both classes. Based on the structure of L-lysine complexed with *Pyrococcus horikoshii* class I LysRS (LysRS1), and homology to glutamyl-tRNA synthetase (GluRS), residues implicated in amino acid recognition and noncognate substrate discrimination were systematically replaced in *Borrelia burgdorferi* LysRS1. The catalytic efficiency of steady-state aminoacylation (k_{cat}/K_M) with lysine by LysRS1 variants fell by 1–4 orders of magnitude compared to wild-type. Disruption of putative hydrogen-bonding interactions through replacement of G29, T31 and Y269 caused up to 1500-fold reductions in k_{cat}/K_M, similar to changes previously observed for comparable variants of class II LysRS (LysRS2). Replacements of W220 and H242, both of which are implicated in hydrophobic interactions with the side chain of lysine, resulted in more dramatic changes with up to 40,000-fold reductions in k_{cat}/K_M observed. This indicates that the more compact LysRS1 active site employs both electrostatic and hydrophobic interactions during lysine discrimination, explaining the ability of LysRS1 to discriminate against noncognate substrates accepted by LysRS2. Several of the LysRS1 variants were found to be more specific than wild-type with respect to noncognate amino acid recognition but less efficient in cognate aminoacylation. This indicates that LysRS1 compromises between efficient catalysis and substrate discrimination, in contrast to LysRS2 which is considerably more effective in catalysis but is less specific than its class I counterpart.

Aminoacyl-tRNAs (aa-tRNAs) are synthesized when an amino acid is esterified to the 3′-end of a transfer RNA (tRNA) (1;2). After their synthesis, aa-tRNAs are screened for their correct pairing by elongation factor–TU (3) and taken to the ribosome where they base pair with the complementary mRNA and participate in protein synthesis. Correctly aminoacylated tRNAs are essential for the faithful translation of mRNA into the encoded polypeptide sequence. The aa-tRNAs are synthesized primarily by the aminoacyl-tRNA synthetases (aaRS) (4). The accuracy of aa-tRNA synthesis is ensured by the extremely high substrate specificity of the aaRSs, and this is further enhanced in some synthetases by the existence of editing mechanisms directed against noncognate substrates (5). The 20 aaRS proteins, as for example found in *Escherichia coli*, are divided into two mutually exclusive structural groups, comprised of ten members each, termed class I and class II (6–8). The assignment of an aaRS specific for a particular amino acid to one or the other structural class is almost completely conserved. The

†This work was supported by Grant GM 65183 from the National Institutes of Health

*Correspondence to: Dr. Michael Ibba, Department of Microbiology, The Ohio State University, 484 West 12th Avenue, Columbus, Ohio 43210-1292, Phone: 614-292-2120, Fax: 614-292-8120, e-mail: ibba.1@osu.edu.
§Present address: Division of Radiobiology, Department of Radiology, The Ohio State University, Columbus, Ohio 43240, USA

[1]**Abbreviations:** aa-tRNA, aminoacyl-tRNA; aaRS, aminoacyl-tRNA synthetase; AEC, S-(2-aminoethyl)-L-cysteine; LysRS, lysyl-tRNA synthetase.

only widespread exception to this rule is the lysyl-tRNA synthetases (LysRSs). These are class I enzymes (LysRS1) in certain bacteria and archaea but are otherwise members of class II (LysRS2) (9–11). The class I LysRS is found in a number of pathogenic bacteria (e.g. *Borrelia*, *Treponema*, and *Rickettsia* species), and is fundamentally different from the human class II enzyme, suggesting it may be a useful antimicrobial target (12;13).

The existence of both class I and class II-type LysRSs indicates that exactly the same activity (lysylation of $tRNA^{Lys}$) has been achieved in two completely different structural frameworks by convergent evolution. The continued retention of both forms of LysRS prompted investigation of possible biochemical differences between the two enzymes. *In vitro* studies revealed variation in recognition of both the anticodon and acceptor stem of $tRNA^{Lys}$ by LysRS1 and LysRS2 (14–16), but these differences were found to be less significant *in vivo* (17). In contrast, structural differences between their active sites for lysine lead to significantly divergent patterns of noncognate amino acid discrimination by LysRS1 and LysRS2 both *in vitro* and *in vivo* (18). The lysine-binding pocket appears more open in LysRS2 than in LysRS1, and as a result lysine analogues such as S-(2-aminoethyl)-L-cysteine (AEC) are efficient substrates for the class II, but not the class I, enzyme *in vitro*. LysRS1 imparts resistance to growth inhibition by AEC as a result of the difference in noncognate amino acid recognition compared to LysRS2, illustrating how LysRS distribution can contribute to quality control during protein synthesis.

High resolution crystal structures are available for both LysRS1 and LysRS2 in complexes with lysine (19;20). Comparison of the LysRS1 and LysRS2 substrate complexes revealed that while the mechanisms of recognition of the R-group of L-lysine rely on similar arrangements of amino acids in each binding pocket, the active sites are different. Based on the structure of L-lysine complexed with *E.coli* LysRS2 (*lysS*), residues implicated in amino acid recognition and discrimination were systematically replaced and the resulting variants characterized (21). This revealed that LysRS2 predominantly recognizes lysine via hydrogen-bonding interactions with a series of charged residues in the active site. Manipulation of the amino acid binding site allowed up to a four-fold improvement in AEC discrimination by LysRS2, but did not rival the highly effective discrimination of noncognate substrate by LysRS1. These findings suggest fundamentally different roles in substrate discrimination for the conserved aromatic residues found in the two LysRS active sites. To compare substrate selection and discrimination at the two different LysRS active sites, we have now investigated the role of each residue implicated in lysine binding by LysRS1. Comparisons to previous studies indicate that while both enzymes employ a network of hydrogen-bonding interactions to bind lysine, LysRS1 employs an additional network of hydrophobic interactions absent in LysRS2. The impact of this extended substrate binding network on noncognate amino acid recognition suggests that it may directly account for the increased substrate specificity of LysRS1 compared to LysRS2.

EXPERIMENTAL PROCEDURES

Bacterial strains and plasmids

Borrelia burgdorferi lysK encoded LysRS1 cloned into the pET15b vector was used as a template for development of LysRS1 variants. Sets of two complementary primers with 27 nucleotides were designed to encode each desired point mutation. The LysRS1 variants used here were: G29A, T31S, T31G, E43N, G43I, W220L, W220A, W220Y, H242A, H242L, H242W, Y269F, Y269S. PCR reactions using *Pfu* turbo DNA polymerase (Stratagene) were performed according to the manufacturer's procedure. PCR products and pET15b vector were digested with *NdeI* and *BamHI* (New England BioLabs), then ligated and transformed into DH5α cells. Point mutations were confirmed by sequencing each gene completely. *In vitro* transcribed *B. burgdorferi* $tRNA^{Lys}$ (UUU anticodon) was prepared and purified as described before (18).

Lysyl-tRNA synthetase purification

The *B. burgdorferi lysK* encoded LysRS1 and mutants cloned into the pET15b vector were expressed in *E. coli* BL21(DE3) cells as described previously (18). Cells were harvested by centrifugation and washed in column buffer (20 mM Tris-HCl, pH 8, 300 mM NaCl, 30 mM Imidazole, 1 mM $MgCl_2$, 10% glycerol). Cells were resuspended in column buffer supplemented with protease inhibitor (Hoffman-La Roche), passed through a French pressure cell, and then centrifuged at 25000*g* for 30 min. The resulting supernatant was loaded onto a nickel affinity bead column (QIAGEN). Protein was eluted from the nickel affinity column in a buffer of 50 mM Tris-HCl (pH 8), 1 mM $MgCl_2$, 300 mM NaCl, 250 mM Imidazole, 10% glycerol, and 10 mM 2-mercaptoethanol. The fractions containing LysRS1 were pooled and then concentrated by ultrafiltration using an Amicon Ultra-15 unit (Millipore). The concentrated LysRS1 was further loaded onto a Superose 6 column (Amersham Pharmacia Biotech), and eluted in a buffer of 50 mM Hepes (pH 7.2), 25 mM KCl, 10 mM $MgCl_2$, 10% glycerol, and 5 mM 2-mercaptoethanol. The fractions containing LysRS1 were again concentrated by ultrafiltration and stored at −80 C. The concentration of LysRS1 was determined by the Bradford dye-binding procedure using the Bio-Rad Protein Assay system (Bio-Rad).

Aminoacylation assays

Aminoacylation was performed at 37 °C in 100 mM Hepes (pH 7.2), 25 mM KCl, 10 mM $MgCl_2$, 5 mM DTT, 5 mM ATP, 16 μM tRNALys and 50 nM – 5 μM LysRS1. For L-Lys K_M determination, all the concentrations were fixed except for [^{3}H]-L-Lys (L-[U-^{3}H] lysine, 91.0 Ci/mmol, Amersham Corporation), which was added at concentrations varying between 0.2 – 5-fold K_M. The same procedure was followed for tRNA and ATP K_M determinations, in which tRNA or ATP were added at concentrations varying between 0.2 and 5-fold K_M. Nine or 18μL aliquots were taken every 30 s – 15 min and spotted onto 3MM filter disks presoaked in 5% TCA (w/v) containing 0.5% (w/v) [^{12}C]-L-Lys. Sample disks were washed and radioactivity counted as described previously (18). The steady-state kinetic parameters given represent the average of at least two independent experiments where values deviated by no more than 10% between individual determinations.

K_i determination

In order to determine the K_i for S-(2-aminoethyl)-L-cysteine (AEC), at least five different concentrations of the analog were first screened in the aminoacylation reaction for each variant under standard conditions with K_M concentrations of [^{14}C]-L-Lys for each LysRS1 variant. Analog concentrations were then established at which the initial rate of aminoacylation was decreased by 20–50% when compared with the reaction lacking analog, and these levels used for K_i determinations. The K_is presented represent the average of at least two independent experiments where values deviated by no more than 10% between individual determinations.

tRNA aminoacylation with noncognate amino acids

Synthesis of tRNA^{Lys} [^{32}P]-pA76 transcript was performed as described (22). Briefly, the CCA-3′ end of the tRNA was first removed by treatment of 20 μM of tRNA transcript with 73μg/ml of *Crotalus atrox* venom (Sigma) in a buffer containing 40 mM Na-Gly (pH 9.0) and 10 mM Mg-acetate. The mix was incubated for 2 h at 21°C and phenol/chloroform extracted and ethanol precipitated and finally desalted by gel filtration thru a Sephadex G 25 column (Pharmacia). The CCA-3′ end of the tRNA was reconstituted and radiolabeled by incubation for 10 min at 37 °C with 0.5 μM of the snake venom treated tRNA, in 50 mM Na-Gly (pH 9.0), 10 mM $MgCl_2$, 10 μM CTP, 9 μM ATP, 1μM [α-^{32}P]ATP with 3μg/ml of *E. coli* tRNA-terminal nucleotidyltransferase. The reaction was stopped by addition of 1 volume of phenol and the mixture was gel filtered twice thru a G25 column. As described earlier (23), the

aminoacylation reaction was performed in a 10μl aminoacylation media (see above) containing 5mM of cold amino acids, 5μM of transcript and a trace of radiolabeled tRNA. After 15 min of incubation an aliquot was removed and incubated for 30 min at room temperature with P1 RNAse. The liberated [α-^{32}P]AMP and aminoacyl-[α-^{32}P]AMP were separated by TLC on PEI cellulose and visualized as described earlier (23).

RESULTS

Selection and characterization of LysRS1 variants

The structure of the active site of *P. horikoshii* LysRS1 implicates six residues in lysine binding (Fig. 1a). Of these amino acids, W220 (*B. burgdorferi* LysRS1 numbering) is conserved in all 61 known class I LysRS proteins, while G29 and Y269 only vary in one known example each (Ala in *Nanoarchaeum equitans*, and Phe in uncultured *Archaeon GZfos32E7*). H242, E43, and T31 are also well conserved, as illustrated by the conservation of all of the corresponding residues between the *B. burgdorferi* and *P. horikoshii* proteins (Fig. 1b). *B. burgdorferi* LysRS1 variants were made with the aims of testing the role of each lysine-binding residue in the active site, and investigating conservation of the synonymous residues in the closely related glutamyl-tRNA synthetase (GluRS) active site (Fig. 1b). The G29A replacement was intended to disrupt hydrogen bonding with the α-amino group of lysine; T31S and T31G to displace and disrupt, respectively, hydrogen bonding with the α-carboxyl group; E43Q and E43I to disrupt electrostatic interaction with the ε-amino group; Y269F and Y269S to disrupt hydrogen-bonding with the ε-amino group.

Previous studies and comparisons of the active sites of the other subclass Ib aaRSs, glutaminyl-tRNA synthetase (GlnRS) and GluRS, revealed residues that participate in tRNA-dependent amino acid recognition. Structural (24) and biochemical (25) studies have shown that residues Y211 and F233 of *E. coli* GlnRS stack against the terminal adenosine of $tRNA^{Gln}$ during formation of the glutamine-binding site. A conserved role in other class 1b aaRSs for the residue equivalent to Y211 of GlnRS is suggested by the strict conservation of the analogous position as Tyr in GluRS. Multiple sequence alignments with GluRS show that the analogous position in all known class I LysRS sequences is instead occupied by Trp (W220 in *B. burgdorferi*). Positions analogous to F233 of GlnRS are also fairly well conserved, being His or Trp in GluRS and His or Leu (rarely Ile) in LysRS1 (H242 in *B. burgdorferi*). Therefore, the modifications W220Y and H242W were designed to determine whether protein-RNA stacking interactions affect lysine binding, which would be expected to result in corresponding changes in the kinetic parameters for both lysine and tRNA.

The steady-state kinetic parameters for lysine during aminoacylation were measured for wild-type and LysRS1 variants (Table 1). The catalytic efficiency (k_{cat}/K_M) for lysine compared to wild-type decreased significantly for most variants; the only exceptions being H242L and T31S which both showed almost no change, and Y269F that displayed only a 6-fold drop in efficiency. No aminoacylation was detected using either the filter binding or 3′-labelling assay for E43Q or E43I (Table 1 and Fig. 2), indicating that replacements at this position abolish activity. H242W was also inactive in filter binding assays, but showed slight activity in alternative assays (Fig. 2) indicating that this replacement severely reduces aminoacylation efficiency. The H242A replacement also strongly impacted efficiency (40,000-fold reduction), while H242L caused almost no change. W220A had little effect on K_M, but dramatically reduced k_{cat} (450-fold decrease), while W220Y increased K_M 20-fold, but reduced k_{cat} only 3-fold. Y269F had much less effect on both K_M and k_{cat} than Y269S. Y269F increased K_M 2-fold and decreased k_{cat} 3-fold, while Y269S increased K_M 10-fold and reduced k_{cat} 130-fold. Similarly, T31S had much less effect on both K_M and k_{cat} than T31G. T31S slightly increased both K_M and k_{cat} (3- and 2-fold, respectively), while T31G increased K_M 20-fold and decreased k_{cat} 70-fold.

LysRS1, together with arginyl-tRNA synthetase (ArgRS), GlnRS and GluRS, forms a small sub-group of aaRSs that requires the presence of tRNA for amino acid activation. To investigate whether the observed effects of the various replacements on lysine binding were the indirect results of changes in tRNA binding, the kinetic parameters for $tRNA^{Lys}$ were determined (Table 2). No significant changes compared to wild-type were seen in the K_Ms for tRNA, and the changes in k_{cat} were very similar to those observed for lysine. Comparison of LysRS1 to the closely related GluRS active site suggested that T31 and Y269 might also participate directly in ATP binding. The aminoacylation kinetic parameters for variants containing replacements of T31 and Y269 showed only relatively modest changes in the K_M for ATP (2–7 fold decreases, Table 3), suggesting that the main role of these residues is in lysine binding.

Substrate discrimination by LysRS1 variants

Previous studies indicated that LysRS1 and LysRS2 are markedly different in their abilities to discriminate lysine analogues (18). For example, the competitive inhibitor AEC has a K_i for the aminoacylation reaction that is several hundred-fold lower for LysRS2 than LysRS1. Structural modeling suggested that this difference was in part due to steric hindrance by H242 and W220 in LysRS1, as the comparable region of the LysRS2 active site appears more open. To investigate the structural basis of lysine analogue discrimination by LysRS1, the K_is for AEC of H242 and W220 variants were determined (Table 4). The G29A variant was also investigated in light of its increased discrimination of canonical amino acids (see below). For all the LysRS1 variants tested the k_{cat} did not change significantly in the presence of AEC, indicating that it acted as a competitive inhibitor. With the exception of LysRS1 H232L, the K_i as compared to wild-type increased for all the variants. Comparison to wild-type, the changes in apparent AEC ($K_i/K_i^{w.t.}$) and lysine ($K_M/K_M^{w.t.}$) binding showed that, with the exceptions of W220A and H242L, the various replacements were considerably more detrimental to cognate than noncognate substrate binding. To further investigate the relationship between cognate amino acid recognition and the discrimination of noncognate substrates, we tested the ability of LysRS1 variants to activate canonical amino acids other than lysine.

Aminoacylation of canonical amino acids by LysRS1 variants

Structural studies have previously shown that *P. horikoshii* LysRS1 bears a striking similarity to *T. thermophilus* GluRS that extends throughout the whole structure and includes the active site (20). Detailed comparisons of amino acid binding based on the *P. horikoshii* LysRS1 structure suggest that *B. burgdorferi* LysRS1 residues W220, H242, T31, G29 and E43 most closely correspond to Y187, W209, S9, A7 and I21 in *T. thermophilus* GluRS, respectively. The corresponding LysRS1 variants, where the identities of the appropriate residues were changed to those observed in GluRS, were then tested for their ability to utilize the canonical noncognate amino acids glutamic acid and arginine (Fig. 2). As previously observed (18), wild-type LysRS1 is able to aminoacylate $tRNA^{Lys}$ with both glutamic acid and arginine, albeit at substantially lower levels than with lysine. However, of the LysRS1 variants tested, only T31S retained the ability to utilize glutamic acid and arginine, all the other variants showing no such activities.

DISCUSSION

Specific recognition of lysine in the LysRS1 active site

While comparisons to our previous study of *E. coli* LysRS2 clearly identify residues with similar roles in the class I and II enzymes, it is also evident that the two residues characteristic of the more closed LysRS1 active site are functionally specific for the class I protein. H242 is positioned very close to bound lysine in the structure, and plays an important role in hydrophobic interaction with the substrate. When the potential for this interaction was lost in LysRS1 H242A, this was accompanied by a 40,000-fold drop in catalytic efficiency, while a

conservative substitution that maintained hydrophobicity (H242L) had no effect. The almost complete loss in activity for H242W likely results from the larger indole moiety limiting lysine access to the active site. The proposed role of H242 in contributing to hydrophobic interactions while limiting access to the active site correlates with data from LysRS1 sequence alignments, where this position is conserved as either His or Leu and rarely Ile (there are 45 examples of His, 15 of Leu, and one of Ile, in the 61 known LysRS1 sequences aligned). Initial examination of the active site of LysRS1 suggested similar roles in lysine binding for H242 and W220, but biochemical analyses indicate that they differ in function. The W220L and W220Y replacements both significantly increased the K_M for lysine but W220A had no effect, suggesting that direct interactions with the substrate are not as important at this position as at H242. The changes at W220 may instead affect the position of H242, which is only 3.2 Å away, thereby perturbing both direct interactions with lysine and stacking with A76 and C75 of the tRNA (Fig. 3a). The stacking array is also important for the correct position and orientation of A76 of the tRNA into the active site (in GluRS of *T. thermophilus*, the W220 corresponds to Y187). Disruption of the correct positioning of H242 in the W220A and W220L variants severely impaired the k_{cat}, while W220Y resulted in almost no changes in catalytic efficiency. The predicted effect of W220 substitutions would be to impair tRNA binding since the correct positioning of the stacking array would be compromised. However, no variation in K_M for tRNA was observed for modifications of W220 which suggests this residue is not involved in the same direct interactions with A76 as the corresponding Y187 in GluRS. Nevertheless, further studies are now needed to determine the extent to which interactions between W220 and H242 and $tRNA^{Lys}$ might contribute to amino acid recognition and catalysis through local conformational adjustments of the active site.

The crystal structure of *P. horikoshii* LysRS1 suggests that Y268 may be too far away from the ε-amino group of lysine to allow strong interaction with it through hydrogen-bonding. Instead, comparison to other tRNA-dependent class I aaRSs indicates that Y268 is in a hydrophobic pocket and is able to bind the adenine portion of ATP through stacking interactions (Fig. 3b). Superposition of GluRS, ArgRS and LysRS1, using the C-α backbones to search for similar structural motifs, shows that in ArgRS the same position is occupied by the conserved residue F402 which can also stack against ATP (Fig. 3b). The decreases in catalytic efficiency for Y269S LysRS1 (1600-fold for lysine and 5900-fold for ATP) confirmed that the aromatic ring of Tyr is important for interaction with ATP. In agreement with a role in stacking at this position, Y269F showed almost no reduction in K_M for any of the substrates and only a small drop in k_{cat}. Thus, rather than Y269 being directly involved in lysine binding, this residue is instead involved in the correct positioning of ATP by stacking with the adenosine moiety. This contrasts with the most analogous residue in LysRS2, Y280, which instead interacts directly with lysine.

Kinetic analyses indicated that the role of G29 in LysRS1 involves hydrogen-bonding with the α-amino group of lysine. The increase in K_M with almost no change in k_{cat} for lysine indicated that G29 in LysRS1 performs the same function as G216 in LysRS2 of *E.coli.* Another prediction, that T31 is involved in hydrogen-bond interactions with the α-carboxylate group of lysine, was confirmed by the replacement T31G which caused a decrease in specific activity of this enzyme while T31S exhibited almost the same kinetic parameters as wild-type. The docking model (Fig. 3b) indicated that T31 also forms a hydrogen-bond with the oxygen atom from the α-phosphate of ATP. The corresponding position in *T. thermophilus* GluRS, S9, is involved in hydrogen-bonding with the oxygen atom from the α-phosphate of ATP. The kinetics for ATP indicated that T31G affected the correct positioning and possible orientation of ATP in the active site. The substitution T31S had no effect on the kinetic parameters for lysine or ATP, indicating that the conservation of H-bonding capacity at this position among the classIb aaRSs is important for interaction with ATP.

Substrate specificity determinants in LysRS1

The enhanced discrimination of lysine analogues and noncognate amino acids by LysRS1 was predicted to be based on the compactness of its active site when compared to LysRS2 (18). In our previous model, we proposed that H242 and W220 would sterically hinder AEC binding in the active site of LysRS1. Substitutions of H242, W220 and G29 showed that any changes to the active site that compromise lysine binding also affect AEC, as also seen for similar replacements in LysRS2 (21). W220A is the only replacement to show almost no effect on the K_M for lysine but a large increase in the K_I for AEC, suggesting that the absence of the bulky indole moiety promotes closure of the active site thereby further hindering the binding of AEC.

Investigation of the effect of synonymous residues conserved within GluRS and LysRS1 on the discrimination of noncognate amino acids indicated that the active site is fine tuned to compromise between efficiency and specificity. Almost all the replacements severely reduced efficiency (k_{cat}/K_M for lysine) but increased specificity as they lost the ability to charge $tRNA^{Lys}$ with glutamic acid and arginine. Both glutamic acid and arginine are used by the wild-type enzyme but only the variant T31S, a conserved replacement with little loss in lysine efficiency, could also charge the noncognate substrates. Any attempts to replace residues involved in lysine binding and convert the LysRS1 active site into a form more similar to GluRS caused severe decreases in lysine binding and a complete loss in glutamic acid and arginine binding. Thus, despite the residual structural and mechanistic similarities between LysRS1 and GluRS, both have diverged sufficiently to maximize binding and selectivity for cognate amino acids while excluding noncognate amino acids within very similar active site architectures.

Divergent mechanisms of substrate discrimination in LysRS1 and LysRS2

The evolution of two unrelated structures to perform the same reaction is so far limited to LysRS among the aaRSs. We previously proposed that the active site of LysRS2 is more open and, therefore, able to accommodate lysine analogues more easily than LysRS1. Our present findings corroborate this idea and further suggest that the binding network in LysRS1 is different than in LysRS2. The kinetic data for W220 and Y269 variants indicate these two residues do not play important roles in lysine binding, but rather form the active site scaffold for interactions with ATP and tRNA. In the LysRS2 structure, lysine binding is mainly based on a complex hydrogen-bonding network and is much more robust (19), as also indicated by biochemical studies (21). The usage of electrostatic interactions and hydrogen-bonds in LysRS2 leads to tight lysine binding (2.6μM) when compared to LysRS1 (225μM), and since the lysine binding network is more extensive, any single mutation in the LysRS2 active site does not cause as dramatic a change in the catalytic efficiency as observed in LysRS1 variants. There is only one LysRS2 replacement (E278D) which causes a reduction of over 1000-fold in k_{cat}/K_M for lysine compared to wild-type, and changes in the active site at the other 7 residues interacting directly with lysine lower catalytic efficiency considerably less. The crystal structure of *P. horikoshii* LysRS1 implicates only 4 residues (E43, H241, T31, G29) that could play important roles in lysine binding. Since fewer residues in the active site of LysRS1 are directly involved in binding and discrimination of lysine, any non-conservative replacement of these residues can cause severe decreases in catalytic efficiency. The lysine binding network in LysRS1 takes advantage of the specific size and positioning of the substrate in the active site with two distinct sides; polar hydrogen-bond interactions with the functional groups of lysine positioned on one side, and hydrophobic interactions with the lysine backbone on the other. This dual interaction contributes to the difference in sensitivity towards the discrimination of lysine analogues by excluding larger analogues such as AEC. The same mechanism is not observed in LysRS2, which efficiently screens for hydrogen-bond interactions within a larger active site thereby allowing inhibition by AEC.

Attempts to explain the evolutionary role of two unrelated LysRSs belonging to class I and class II initially focused on identity elements of the tRNA, since this is the largest and potentially most diverse molecule that the two LysRSs have to discriminate (14). However the subtle differences in $tRNA^{Lys}$ discrimination *in vitro* between LysRS1 and LysRS2, with a G-U wobble in the second base pair of the acceptor stem being an anti-determinant for LysRS2, were not significant *in vivo* (17). Subsequent analyses of lysine analogues demonstrated *in vivo* and *in vitro* that the evolutionary pressure to retain two forms of LysRS likely arose to avoid infiltration of the genetic code by these near-cognate amino acids. The mechanisms of lysine recognition and discrimination by both enzymes are sufficiently different that it was not possible to convert the active site of LysRS2, which is more catalytically efficient, into a more selective site as found in LysRS1 (21). These earlier findings, together with the data presented here, clearly indicate that the continued evolutionary retention of the less efficient class I form of LysRS is a result of the higher substrate specificity offered by the class I active site compared to LysRS2.

Acknowledgements

We thank O. Nureki (Tokyo Institute of Technology) for providing the crystal structure coordinates for L-lysine bound to *P. horikoshii* LysRS1, and C. Hausmann and J. Levengood for critical reading of the manuscript. S.W. is supported by the China Scholarship Program, S.F.A. by an American Heart Association Predoctoral Fellowship.

References

1. Francklyn C, Perona JJ, Puetz J, Hou YM. Aminoacyl-tRNA synthetases: versatile players in the changing theater of translation. RNA 2002;8:1363–1372. [PubMed: 12458790]
2. Ibba M, Söll D. Aminoacyl-tRNAs: setting the limits of the genetic code. Genes Dev 2004;18:731–738. [PubMed: 15082526]
3. Asahara H, Uhlenbeck OC. Predicting the binding affinities of misacylated tRNAs for *Thermus thermophilus* EF-Tu. GTP. Biochemistry 2005;44:11254–11261. [PubMed: 16101309]
4. Ibba M, Becker HD, Stathopoulos C, Tumbula DL, Söll D. The adaptor hypothesis revisited. Trends Biochem Sci 2000;25:311–316. [PubMed: 10871880]
5. Hendrickson, TL.; Schimmel, P. Translation Mechanisms. Lapointe, J.; Brakier-Gingras, L., editors. Kluwer Academic/Plenum Publishers; 2003. p. 34-64.
6. Eriani G, Delarue M, Poch O, Gangloff J, Moras D. Partition of tRNA synthetases into two classes based on mutually exclusive sets of sequence motifs. Nature 1990;347:203–206. [PubMed: 2203971]
7. Cusack S. Aminoacyl-tRNA synthetases. Curr Opin Struct Biol 1997;7:881–889. [PubMed: 9434910]
8. Ribas De Pouplana L, Schimmel P. Two classes of tRNA synthetases suggested by sterically compatible dockings on tRNA acceptor stem. Cell 2001;104:191–193. [PubMed: 11269237]
9. Ibba M, Morgan S, Curnow AW, Pridmore DR, Vothknecht UC, Gardner W, Lin W, Woese CR, Söll D. A euryarchaeal lysyl-tRNA synthetase: resemblance to class I synthetases. Science 1997;278:1119–1122. [PubMed: 9353192]
10. Ambrogelly A, Korencic D, Ibba M. Functional annotation of class I lysyl-tRNA synthetase phylogeny indicates a limited role for gene transfer. J Bacteriol 2002;184:4594–4600. [PubMed: 12142429]
11. Ataide SF, Jester BC, Devine KM, Ibba M. Stationary-phase expression and aminoacylation of a transfer-RNA-like small RNA. EMBO Rep 2005;6:742–747. [PubMed: 16065067]
12. Ibba M, Bono JL, Rosa PA, Söll D. Archaeal-type lysyl-tRNA synthetase in the Lyme disease spirochete *Borrelia burgdorferi*. Proc Natl Acad Sci U S A 1997;94:14383–14388. [PubMed: 9405621]
13. Raczniak G, Ibba M, Söll D. Genomics-based identification of targets in pathogenic bacteria for potential therapeutic and diagnostic use. Toxicology 2001;160:181–189. [PubMed: 11246138]
14. Ibba M, Losey HC, Kawarabayasi Y, Kikuchi H, Bunjun S, Söll D. Substrate recognition by class I lysyl-tRNA synthetases: a molecular basis for gene displacement. Proc Natl Acad Sci U S A 1999;96:418–423. [PubMed: 9892648]

15. Söll D, Becker HD, Plateau P, Blanquet S, Ibba M. Context-dependent anticodon recognition by class I lysyl-tRNA synthetases. Proc Natl Acad Sci U S A 2000;97:14224–14228. [PubMed: 11121028]
16. Ambrogelly A, Frugier M, Ibba M, Soll D, Giege R. Transfer RNA recognition by class I lysyl-tRNA synthetase from the Lyme disease pathogen *Borrelia burgdorferi*. FEBS Lett 2005;579:2629–2634. [PubMed: 15862301]
17. Jester B, Levengood J, Roy H, Ibba M, Devine K. Non-orthologous replacement of lysyl-tRNA synthetase prevents addition of lysine analogs to the genetic code. Proc Natl Acad Sci U S A 2003;100:14351–14356. [PubMed: 14623972]
18. Levengood J, Ataide SF, Roy H, Ibba M. Divergence in noncognate amino acid recognition between class I and class II lysyl-tRNA synthetases. J Biol Chem 2004;279:17707–17714. [PubMed: 14747465]
19. Onesti S, Desogus G, Brevet A, Chen J, Plateau P, Blanquet S, Brick P. Structural studies of lysyl-tRNA synthetase: conformational changes induced by substrate binding. Biochemistry 2000;39:12853–12861. [PubMed: 11041850]
20. Terada T, Nureki O, Ishitani R, Ambrogelly A, Ibba M, Söll D, Yokoyama S. Functional convergence of two lysyl-tRNA synthetases with unrelated topologies. Nat Struct Biol 2002;9:257–262. [PubMed: 11887185]
21. Ataide SF, Ibba M. Discrimination of cognate and noncognate substrates at the active site of class II lysyl-tRNA synthetase. Biochemistry 2004;43:11836–11841. [PubMed: 15362869]
22. Roy H, Ling J, Alfonzo J, Ibba M. Loss of editing activity during the evolution of mitochondrial phenylalanyl-tRNA synthetase. J Biol Chem 2005;280:38186–38192. [PubMed: 16162501]
23. Wolfson AD, Uhlenbeck OC. Modulation of $tRNA^{Ala}$ identity by inorganic pyrophosphatase. Proc Natl Acad Sci U S A 2002;99:5965–5970. [PubMed: 11983895]
24. Rath VL, Silvian LF, Beijer B, Sproat BS, Steitz TA. How glutaminyl-tRNA synthetase selects glutamine. Structure 1998;6:439–449. [PubMed: 9562563]
25. Liu J, Ibba M, Hong KW, Söll D. The terminal adenosine of $tRNA^{Gln}$ mediates tRNA-dependent amino acid recognition by glutaminyl-tRNA synthetase. Biochemistry 1998;37:9836–9842. [PubMed: 9657697]
26. Sekine S, Nureki O, Dubois DY, Bernier S, Chenevert R, Lapointe J, Vassylyev DG, Yokoyama S. ATP binding by glutamyl-tRNA synthetase is switched to the productive mode by tRNA binding. EMBO J 2003;22:676–688. [PubMed: 12554668]
27. Cavarelli J, Delagoutte B, Eriani G, Gangloff J, Moras D. L-arginine recognition by yeast arginyl-tRNA synthetase. EMBO J 1998;17:5438–5448. [PubMed: 9736621]
28. Alexandrov NN. SARFing the PDB. Protein Eng 1996;9:727–732. [PubMed: 8888137]
29. DeLano, WL. The PyMOL Molecular Graphics System. 2002. http://www.pymol.org

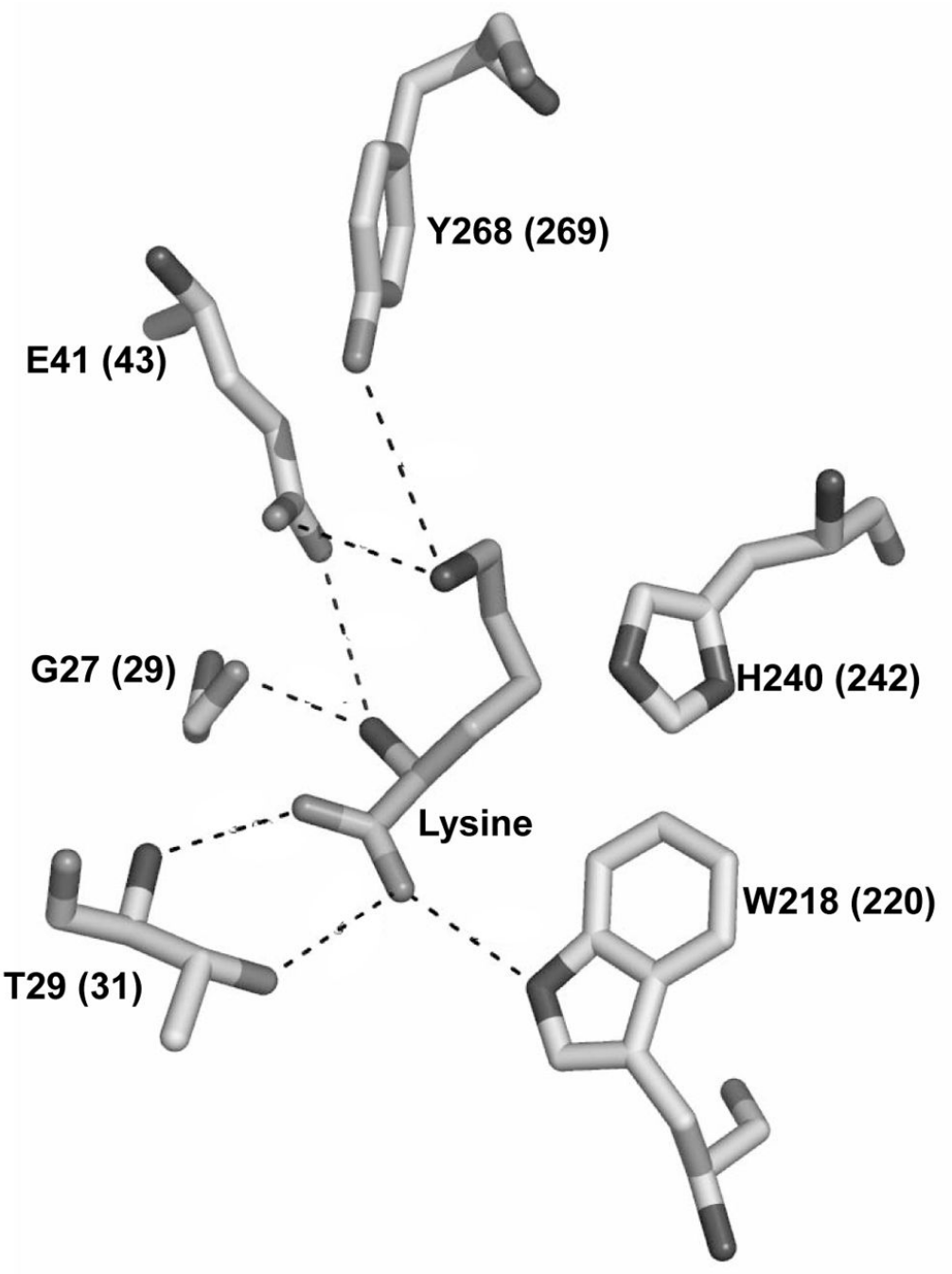

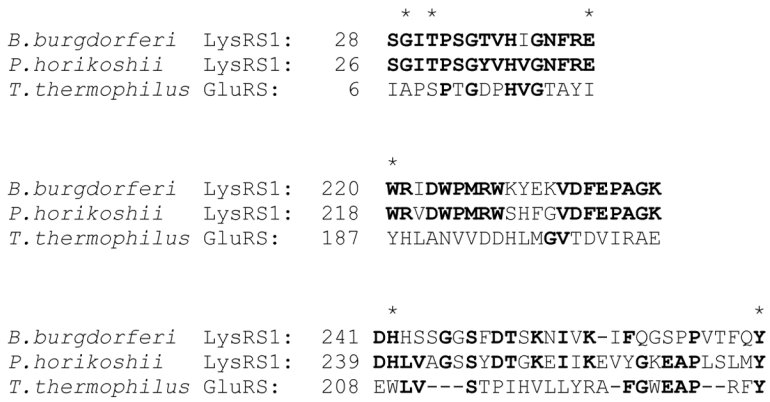

Figure 1.

The active site of *P. horikoshii* LysRS1. **A,** L-lysine in the active site of *P. horikoshii* LysRS1 (adapted from (20)). Hydrogen-bonds are shown as dashed lines, and the numbering of the corresponding positions in *B. burgdorferi* LysRS1 is indicated in parentheses. **B,** alignment of amino acid binding site residues from the *B. burgdorferi* and *P. horikoshii* class I LysRSs, and *T. thermophilus* GluRS. Positions conserved in at least two of the sequences are shown in bold; those replaced in this study are indicated (*).

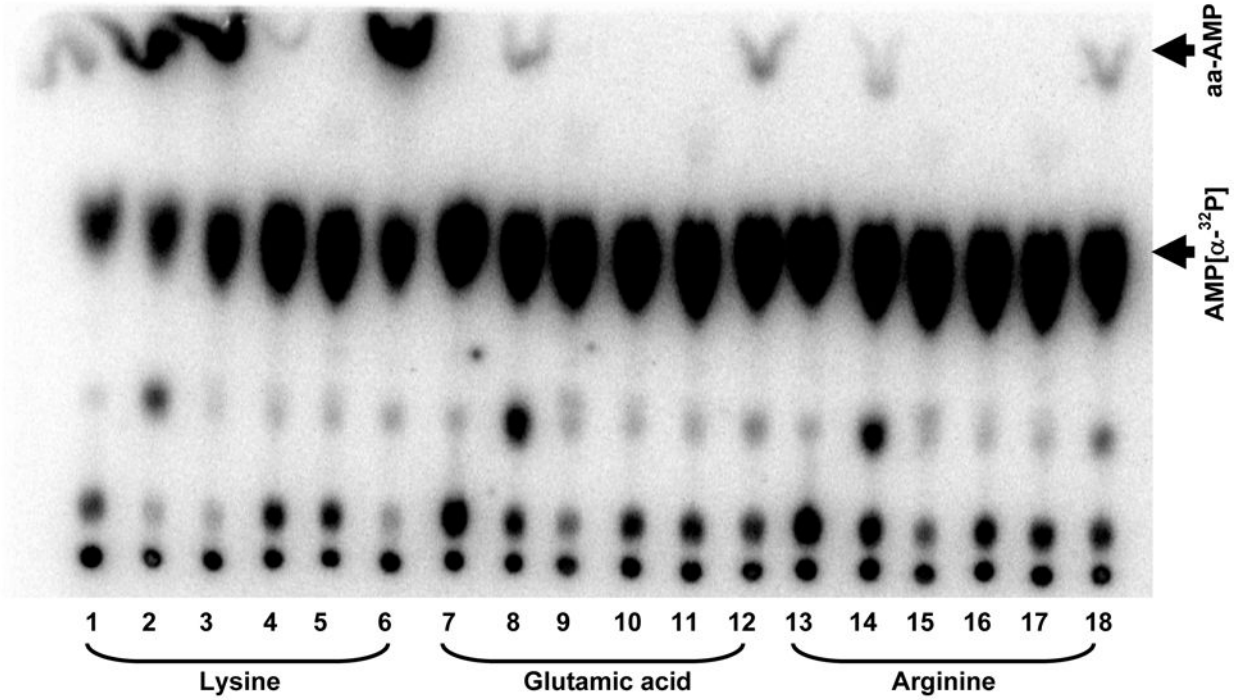

Figure 2.
TLC analysis of $tRNA^{Lys}$ aminoacylation with lysine and noncognate amino acids by wild-type and variant *B. burgdorferi* LysRS1. Lanes 1–6, G29A, T31S, W220Y, H242W, E43I, and wild-type LysRS1, respectively, with lysine. Lanes 7–12, as 1–6 except with glutamic acid instead of lysine. Lanes 13–18, as 1–6 except with arginine instead of lysine.

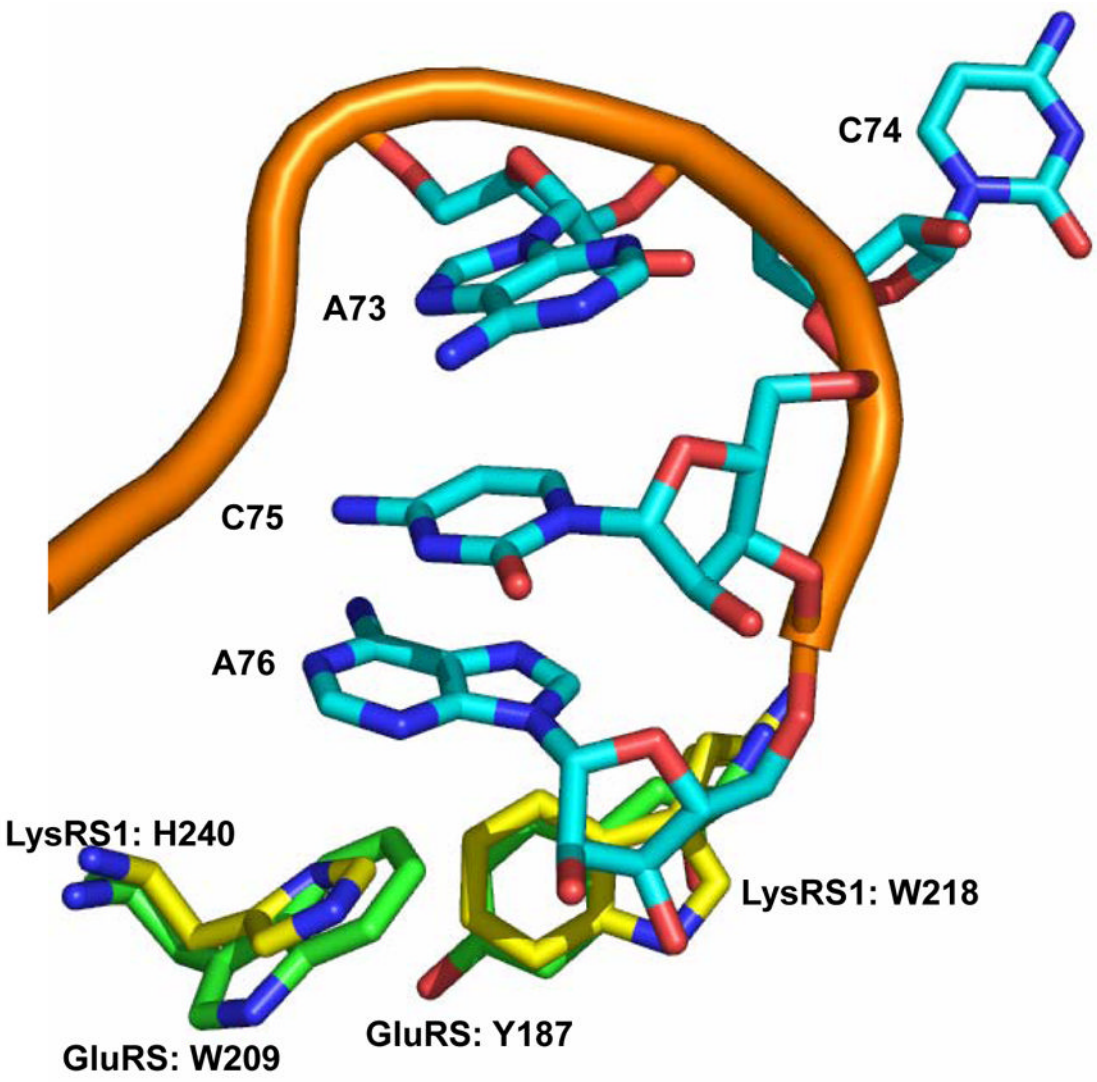

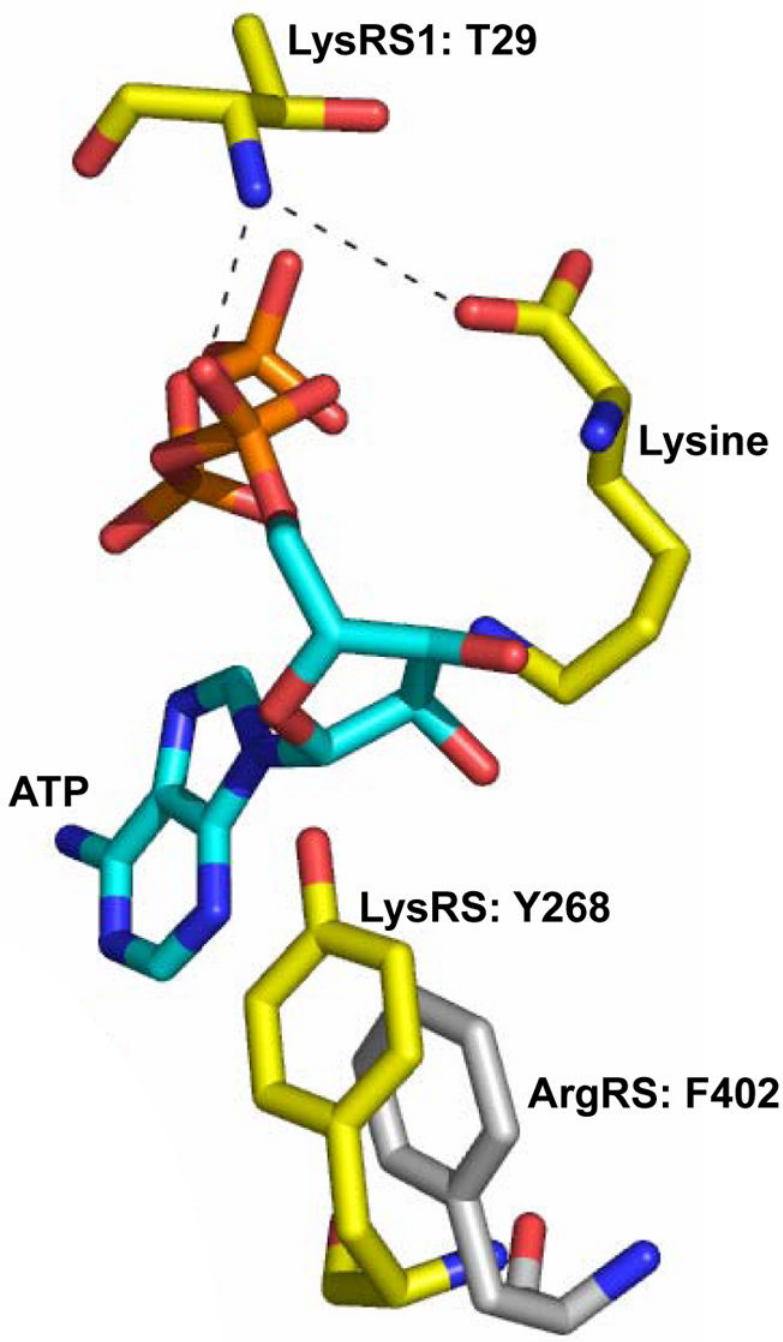

Figure 3.

A, detail of the superposition of the structures of *P. horikoshii* LysRS1 (31) and the *T. Thermophilus* GluRS:tRNA^{Glu} complex (26). The 3′-end of tRNA^{Glu} is shown in cyan with the phosphate backbone in orange, the GluRS active site residues Tyr187 and Trp209 are shown in green, and the corresponding LysRS1 residues Tyr218 and His 240 are shown in yellow. **B,** detail of the superposition of the structures of the active sites of *P. horikoshii* LysRS1, the GluRS:ATP complex of *T. Thermophilus* (26) and yeast ArgRS (27). LysRS1 residues are shown in yellow, GluRS in green, and ArgRS in gray. The positions of substrates, L-lysine for LysRS1 and L-glutamic acid:ATP for GluRS, are also indicated. Structure superpositions were

made using the software SARF2 (28) to search for similar structural motifs based on Cα-backbones, and subsequently visualized with PyMOL (29).

Table 1

Steady-state aminoacylation kinetics of wild-type and variant *B. burgdorferi* LysRS1 with lysine.

LysRS	K_M (mM)	k_{cat} (s^{-1})	k_{cat}/K_M (R)[a]
Wild-type	0.230 ± 0.02	0.34 ± 0.009	1
G29A	6.3 ± 0.50	0.45 ± 0.1	20
T31G	4.4 ± 0.7	0.0046 ± 0.0003	1400
T31S	0.76 ± 0.07	0.53 ± 0.03	2
E43Q	Nd[b]		
E43I	Nd		
W220A	0.330 ± 0.04	0.00075 ± 0.00004	650
W220L	3.3 ± 0.6	0.00017 ± 0.00001	29000
W220Y	4.7 ± 0.4	0.13 ± 0.05	50
H242A	3.3 ± 0.9	0.00012 ± 0.00001	40000
H242L	0.18 ± 0.01	0.29 ± 0.008	0.9
H242W	Nd		
Y269F	0.40 ± 0.04	0.099 ± 0.003	6
Y269S	2.8 ± 0.3	0.0026 ± 0.0001	1600

[a] Relative decrease compared to wild-type.

[b] No detectable activity.

Table 2

Steady-state aminoacylation kinetics of wild-type and variant *B. burgdorferi* LysRS1 with $tRNA^{Lys}_{UUU}$.

LysRS	K_M (μM)	k_{cat} (s^{-1})	k_{cat}/K_M (R)[a]
Wild-type	2.0 ± 0.1	0.33 ± 0.005	1
G29A	5.1 ± 0.3	0.59 ± 0.015	1.4
T31G	2.1 ± 0.1	0.0050 ± 0.0001	50
T31S	2.1 ± 0.2	0.68 ± 0.02	0.5
E43Q	Nd[b]		
E43I	Nd		
W220A	2.5 ± 0.2	0.00056 ± 0.00002	740
W220L	1.1 ± 0.1	0.00012 ± 0.000003	1500
W220Y	1.2 ± 0.1	0.23 ± 0.006	0.9
H242A	1.0 ± 0.2	0.00013 ± 0.000008	1300
H242L	1.3 ± 0.05	0.29 ± 0.004	0.7
H242W	Nd		
Y269F	0.83 ± 0.1	0.14 ± 0.004	1
Y269S	1.1 ± 0.09	0.0023 ± 0.00006	79

[a] Relative decrease compared to wild-type.

[b] No detectable activity.

Table 3

Steady-state aminoacylation kinetics of wild-type and variant *B. burgdorferi* LysRS1 with ATP.

LysRS	K_M (mM)	k_{cat} (s^{-1})	k_{cat}/K_M (R)[a]
Wild-type	1.3 ± 0.4	0.57 ± 0.09	1
T31G	9.5 ± 2	0.0011 ± 0.0002	3800
T31S	1.7 ± 0.3	1.7 ± 0.2	0.4
Y269F	1.6 ± 0.3	0.017 ± 0.002	40
Y269S	6.9 ± 0.4	0.00051±0.00006	5900

[a] Relative decrease compared to wild-type.

Table 4

Kinetic parameters for the inhibition of steady-state aminoacylation by wild-type and variant *B. burgdorferi* LysRS1 in the presence of AEC.

LysRS	K_i (mM)	k_{cat} (s^{-1})	$K_i/K_i^{w.t.}$	$K_M/K_M^{w.t.}$
Wild-type	3.6 ± 0.2	0.32 ± 0.006	1	1
W220A	19 ± 2	0.00082 ± 0.00003	5	1
W220L	11 ± 1	0.00024 ± 0.000003	3	14
W220Y	17 ± 1	0.15 ± 0.003	5	20
H242A	8.5 ± 1	0.00016 ± 0.000005	2	14
H242L	2.9 ± 0.3	0.36 ± 0.01	1	1
G29A	11.8 ± 2	0.40 ± 0.02	3	30